New Codes on Graphs Constructed by Connecting Spatially Coupled Chains

Truhachev, Dmitri; Mitchell, David G.M.; Lentmaier, Michael; Costello Jr., Daniel J.

Published in:
2012 Information Theory and Applications Workshop

DOI:
10.1109/ITA.2012.6181771

2012

New Codes on Graphs Constructed by Connecting Spatially Coupled Chains

Dmitri Truhachev*, David G. M. Mitchell†, Michael Lentmaier‡, and Daniel J. Costello, Jr.†
*Department of Computing Science, University of Alberta, Edmonton, Canada
dmitryt@ualberta.ca
†Dept. of Electrical Engineering, University of Notre Dame, Notre Dame, Indiana, USA,
{david.mitchell, costello.2}@nd.edu
‡Vodafone Chair Mobile Communications Systems, Dresden University of Technology, Dresden, Germany,
michael.lentmaier@ifn.et.tu-dresden.de

***Abstract*—A novel code construction based on spatially coupled low-density parity-check (SC-LDPC) code chains is presented. The proposed code ensembles are described by graphs in which individual SC-LDPC code chains of various lengths serve as edges. We demonstrate that connecting several appropriately chosen SC-LDPC code chains results in improved iterative decoding thresholds compared to those of a single coupled chain in addition to reducing the decoding complexity required to achieve a specific bit error probability.**

I. Introduction

Low-density parity-check (LDPC) block codes, invented by Gallager in the 1960's [1] and later rediscovered in the 1990's, still attract a lot of attention in the communications research community as well as for telecommunication standards development due to their remarkable performance. The iterative decoding techniques generally employed for LDPC decoding are suboptimal compared to optimal maximum likelihood (ML) decoding, which is prohibitively complex for the operational lengths typical of LDPC codes. As a result, the limits of iterative decoding (iterative decoding thresholds) of LDPC block codes are below their ML decoding thresholds.

It has been shown, however, that the asymptotic iterative decoding performance of LDPC convolutional codes (LDPC-CCs), proposed in [2], coincides with the optimal ML decoding performance of closely related LDPC block codes. The explanation for this behavior is the phenomenon of spatial graph coupling that defines the structure of the LDPC-CCs. The principle of spatial graph coupling works in the following way. The Tanner graph of an initial small block code is duplicated a number of times to produce a sequence (chain) of identical graphs. The neighboring copies of the initial graph are then connected by a set of edges. Iterative decoding progresses through the spatially coupled (SC) chain starting from each end. Parity check nodes in the graph copies located at the ends of the chain are connected to a smaller number of variable nodes. As a result, groups of nodes at the ends of the chain form stronger sub-codes and the reliable information propagates through the chain. It has been shown that the iterative decoding thresholds of such SC-LDPC codes coincide with the ML decoding thresholds of the underlying graphs [12] [9], which can be close to the Shannon limit. The principle of spatial graph coupling has attracted significant attention and has been successfully applied in many other areas of communications and signal processing [3], [14], [5].

This work was partially supported by NSF grant CCF08-30650 and the Alberta Innovates Fund.

In this work, we demonstrate that graph coupling need not be limited to simply connecting the component graphs into a single chain. Indeed, the principle of spatial graph coupling can be extended to more general structures. In particular, we propose novel protograph ensembles, in which single SC-LDPC graph chains form the edges, i.e., we construct new codes by interconnecting SC-LDPC chains. We demonstrate that the chain interconnection can result in improved iterative decoding thresholds and decrease the decoding complexity required to achieve specific decoding error probabilities in the near threshold region. We consider communication over the binary erasure channel (BEC) and the additive white Gaussian noise (AWGN) channel, present several connected code constructions, and give insights into the reasons for the obtained performance improvements.

II. Code Construction

We start by considering a regular coupled SC-LDPC code ensemble. Without loss of generality, we demonstrate our approach on an ensemble of coupled $(3, 6)$-regular LDPC codes, constructed by means of protographs [16]. A protograph representing a SC-LDPC code ensemble is a small bipartite graph connecting a set of variable nodes to a set of parity check nodes. Note that a protograph is different from the Tanner graph of a particular LDPC code since every node of a protograph represents a set of M nodes in the Tanner graph of a particular code, and every edge represents a set of M edges. The individual codes (members of the ensemble) are obtained via all possible permutations of these M edges. As such, they are represented by the same protograph. Therefore, a protograph with a *lifting factor* of M describes an ensemble of LDPC codes.

A protograph of a terminated $(3, 6)$-regular SC-LDPC chain of length $L = 8$ is depicted in Fig. 1(a). The green circles in the figure illustrate check nodes and the black circles illustrate variable nodes. Note that each variable node is connected to 3 parity check nodes, while the parity check nodes in the middle are connected to 6 variable nodes. The check nodes located at the beginning and at the end of the chain, however, are only connected to either 2 or 4 variable nodes. A simplified illustration of the $(3, 6)$-regular SC-LDPC length $L = 8$ chain is given in Fig. 1(b). Each magenta node illustrates a segment consisting of one check node and two variable nodes. The

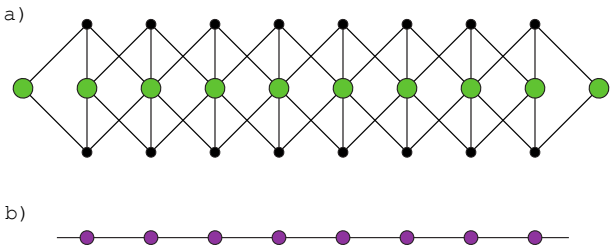

Fig. 1. A spatially coupled $(3, 6)$ protograph chain of length $L = 8$ (a) and its simplified representation (b).

associated incidence matrix $\mathbf{B}$ of the protograph presented in Fig. 1(a) is called the *base* matrix and is given by

$$\mathbf{B} = \begin{bmatrix} 1 & 1 & 0 & 0 & 0 & 0 & 0 & 0 & 0 & 0 & 0 & 0 & 0 & 0 & 0 \\ 1 & 1 & 1 & 1 & 0 & 0 & 0 & 0 & 0 & 0 & 0 & 0 & 0 & 0 & 0 \\ 1 & 1 & 1 & 1 & 1 & 1 & 0 & 0 & 0 & 0 & 0 & 0 & 0 & 0 & 0 \\ 0 & 0 & 1 & 1 & 1 & 1 & 1 & 1 & 0 & 0 & 0 & 0 & 0 & 0 & 0 \\ 0 & 0 & 0 & 0 & 1 & 1 & 1 & 1 & 1 & 1 & 0 & 0 & 0 & 0 & 0 \\ 0 & 0 & 0 & 0 & 0 & 0 & 1 & 1 & 1 & 1 & 1 & 1 & 0 & 0 & 0 \\ 0 & 0 & 0 & 0 & 0 & 0 & 0 & 0 & 1 & 1 & 1 & 1 & 1 & 1 & 0 \\ 0 & 0 & 0 & 0 & 0 & 0 & 0 & 0 & 0 & 0 & 1 & 1 & 1 & 1 & 1 \\ 0 & 0 & 0 & 0 & 0 & 0 & 0 & 0 & 0 & 0 & 0 & 1 & 1 & 1 & 1 \\ 0 & 0 & 0 & 0 & 0 & 0 & 0 & 0 & 0 & 0 & 0 & 0 & 0 & 1 & 1 \end{bmatrix}.$$

The $(3, 6)$-regular SC-LDPC protograph chain ensemble of length L is denoted by $\mathcal{C}(3, 6, L)$.

A. Two Connected Chains (The Loop)

We illustrate one method of constructing more general protographs from SC-LDPC protograph chains using an example (depicted in Fig. 2). The resulting structure, called the loop ensemble and denoted by $\mathcal{L}(3, 6, L)$, consists of two connected $(3, 6)$ SC-LDPCC chains of length L. The last segment of the first chain is connected to an inner segment of the second chain, while the first segment of the second chain is connected to an inner segment of the first chain.

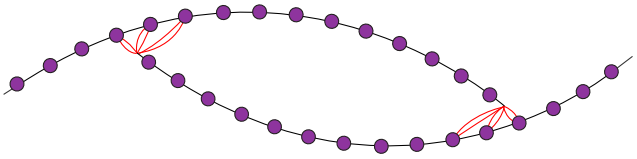

Fig. 2. Two $(3, 6)$ protograph chains of length $L = 15$ connected.

Each of the two connections are made as illustrated in Fig. 3. Fig. 3 (a) presents the connection pattern of the two chains in detail, while Fig. 3 (b) shows a simplified illustration of the connection. Recall that a parity check node located at the beginning of a $(3, 6)$-regular SC-LDPC protograph chain has only two outgoing edges, while the parity check node next to it has only four outgoing edges (instead of 6). Consequently four extra edges are added to the first check node and connected to variable nodes in the other chain. Similarly, two extra edges are added to the second check node to connect it to the variable nodes in the other chain.

We note that the sides of the inner loop of the $\mathcal{L}(3, 6, L)$ protograph each have size $2L/3$. The last node of each chain

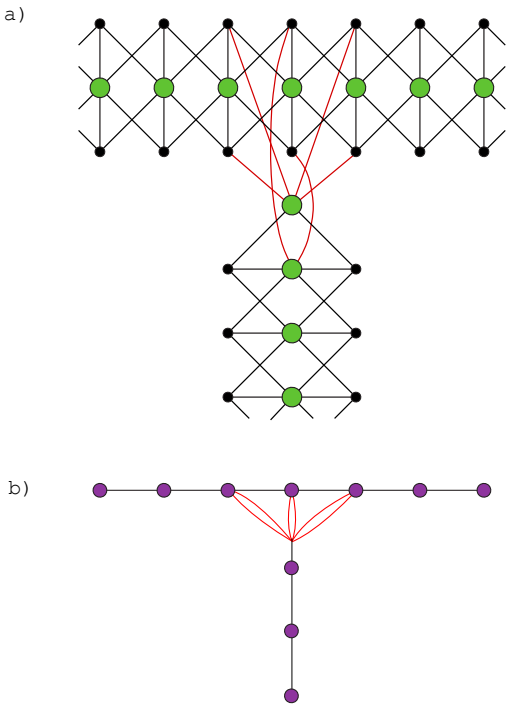

Fig. 3. Two connected spatially coupled $(3, 6)$-regular protograph chains. The connecting edges are shown in red.

is connected to nodes at positions $L/3-1$, $L/3$, and $L/3+1$. Thus, the connection happens at the point that splits the length L chain in proportions $(2L/3, L/3)$. These proportions have been carefully chosen to give the best iterative decoding threshold. For comparison, Fig 4 shows an alternative loop ensemble denoted $\mathcal{L}'(3, 6, L)$, with the chain connected such that the loop proportions are $(L/2, L/2)$. The ensemble $\mathcal{L}'(3, 6, L)$ will be later analyzed and compared to $\mathcal{L}(3, 6, L)$.

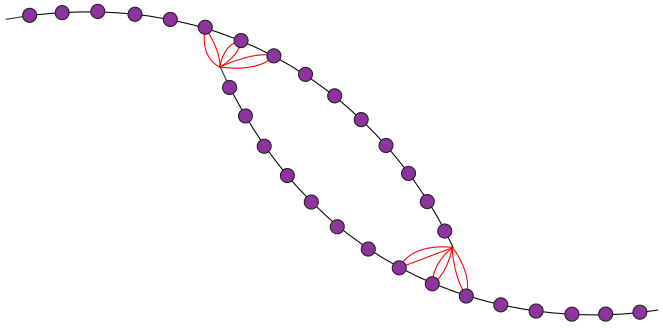

Fig. 4. Alternative loop ensemble $\mathcal{L}'(3, 6, 15)$ with loop proportions $(\lceil L/2 \rceil, \lceil L/2 \rceil)$.

B. The Triangle

The triangle ensemble $\mathcal{T}(3, 6, L)$ (see Fig. 5) is constructed by extending the loop construction to connect three single $(3, 6)$ regular SC-LDPC chains. The chains are connected

to each other at the points $L/3$, similar to the $\mathcal{L}(3,6,L)$ ensemble.

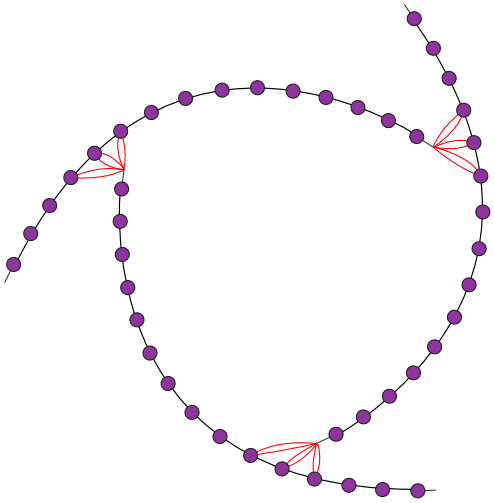

Fig. 5. Three $(3,6)$ protograph chains of length $L=15$ connected to form the triangle ensemble $\mathcal{T}(3,6,L)$.

C. The Mixed Loop

Finally, we consider an example of a "mixed loop" protograph, obtained by connecting a $(3,6)$-regular SC-LDPC chain of length L to a $(4,8)$-regular SC-LDPC chain of the same length. We denote this ensemble, illustrated in Fig. 6, by $\mathcal{L}_1(3,6,4,8,L)$. The $(4,8)$ chain is shown by orange circles in the figure. The end of each chain is connected to the inner parts of the other chain around the node position $L/3$. The last check node of the $(4,8)$ chain has only 2 outgoing edges, the next to last check node has 4, and the second to last check node has only 6 edges. Thus there are 12 new edges which can be used for connecting the end of the $(4,8)$ chain to the $(3,6)$ chain. The connection pattern, shown inside a green circle in Fig. 6, is detailed in Fig. 7.

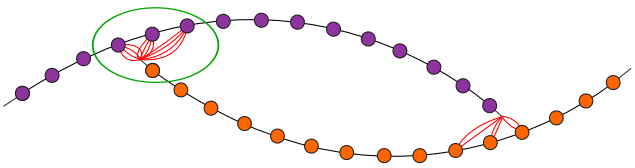

Fig. 6. A $(3,6)$ protograph chain of length $L=15$ connected (magenta) is connected to a $(4,8)$ protograph chain of the same length (orange) to form the ensemble $\mathcal{L}_1(3,6,4,8,L)$.

It will be demonstrated later that, for the case of the mixed ensembles, the spreading of the edge connections is an important design parameter. To illustrate this, we consider an alternative mixed loop ensemble $\mathcal{L}_2(3,6,4,8,L)$, presented in Fig. 8. The 12 edges connecting the end of the $(4,8)$ chain to the $(3,6)$ chain are spread along the $(3,6)$ chain. In particular, the last check node of the $(4,8)$ chain is connected to the nodes at position 13 of the $(3,6)$ chain by 6 edges. The next to last check node of the $(4,8)$ chain is connected to the nodes at position 3 of the $(3,6)$ chain by 4 edges. The second to last check node of the $(4,8)$ chain is connected to the nodes at position 2 of the $(3,6)$ chain by 2 edges.

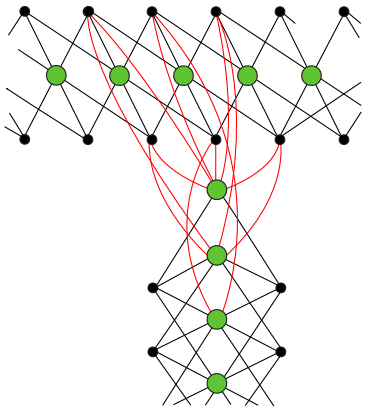

Fig. 7. A detailed illustration of the connection between the end of a $(4,8)$ chain and the inner part of the $(3,6)$ chain in the ensemble $\mathcal{L}_1(3,6,4,8,L)$.

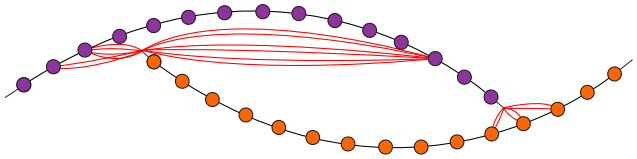

Fig. 8. A $(3,6)$ protograph chain of length $L=15$ (magenta) is connected to a $(4,8)$ protograph chain of the same length (orange) to form the ensemble $\mathcal{L}_2(3,6,4,8,L)$.

III. Analysis of Connected SC-LDPCCs

A. Iterative decoding analysis

In this section we consider communication over a BEC for the example code ensembles. The analysis of the iterative decoding performance of codes described by protographs can be obtained via density evolution and is explained as follows.

We denote the set of variable nodes connected to check node k in the protograph by $\mathbb{V}(k)$ and the set of check nodes connected to variable node j by $\mathbb{C}(j)$. The probability that the message passed from check node k to variable node j in iteration i is an erasure is denoted by $q_{kj}^{(i)}$. The probability of an erasure message from variable node j to check node k is similarly denoted by $p_{jk}^{(i)}$. The following equations relate the erasure probabilities of the messages at different iterations:

$$q_{kj}^{(i)} = 1 - \prod_{j' \in \mathbb{V}(k) \setminus j} (1 - p_{j'k}^{(i-1)}) \ , \tag{1}$$

$$p_{jk}^{(i)} = \epsilon \prod_{k' \in \mathbb{C}(j) \setminus k} q_{k'j}^{(i)} \ . \tag{2}$$

The variable node messages are initialized as $p_{jk}^{(0)} = \epsilon$ at iteration 0. The error probability of the variable nodes at iteration i can be calculated as

$$P_{\mathrm{b}}(j) = \epsilon \prod_{k \in \mathbb{C}(j)} q_{kj}^{(i)} \ . \tag{3}$$

Focusing on a reduction in complexity, we consider simultaneous decoding of the entire code graph, where we employ the updating schedule proposed in [15]. The algorithm designates a target convergence probability $P_{\mathrm{b,max}}$ as well as an update improvement constraint θ. Regular message passing updates are performed for each variable or check node with the following exceptions:

- no update for variable node j is performed if the error probability $P_{\mathrm{b}}(j) < P_{\mathrm{b,max}}$;
- no update for any variable node j or any check node k is performed if all the nodes in $\mathbb{C}(j)$ or $\mathbb{V}(k)$, respectively, were not updated in the previous iteration;
- no update for variable node j is performed if the potential improvement of the bit error probability is less than θ, i.e.,

$$\frac{P_{\mathrm{b,old}}(j) - P_{\mathrm{b,new}}(j)}{P_{\mathrm{b,old}}(j)} < \theta \ . \tag{4}$$

Density evolution provides us with a tool to study the dynamics of the bit error probability behavior at each node of the protograph. Using this tool we attempt to understand the error probability behavior of the connected ensemble, relate it to the ensemble structure, and obtain insight into optimizing connected ensembles. The evolution of the error probability for the variable nodes of the $\mathcal{L}(3, 6, 15)$ ensemble is illustrated in Fig. 9. The red curves, presented in the figure, correspond to the error probability at each node position in the chain at iterations $1, 6, 11, \ldots, 36$ (from top to bottom). The green curves correspond to the error probability as a function of the node position for the single SC-LDPC chain ensemble $\mathcal{C}(3, 6, 15)$ and iteration numbers $1, 6, 11, \ldots, 36$. The BEC erasure probability is fixed to be 0.488. We notice that the red curves display low error probability values much faster than the green curves. In addition, it takes fewer decoding iterations for the ensemble $\mathcal{L}(3, 6, 15)$ to converge to a given error probability value.

Note that each green curve displays a perfect bell shaped figure and is concave. On the other hand, the shape of the red curves is not symmetric. This is due to the fact that the loop protograph comprises two connected chains. The inner part of the 1st chain is connected to the 2nd chain by edges connecting to nodes at positions 4, 5, and 6, shown by red triangles on the figure. The upper red curves dip down at these positions since the connected 2nd chain provides convergence improvement via the connection. On the other hand, the end of the connected chain starts to converge to low probability values slower than for the single chain. This can be observed by comparing to the corresponding green curves. The reason for this behavior is the additional connecting edges which are now present at the end of the 1st chain connecting it to the 2nd. These edges are absent in the single chain case. However, the convergence at the end of the 1st chain improves with iterations as the 2nd chain starts to converge. Finally, the lower red curve displays a perfect bell shape.

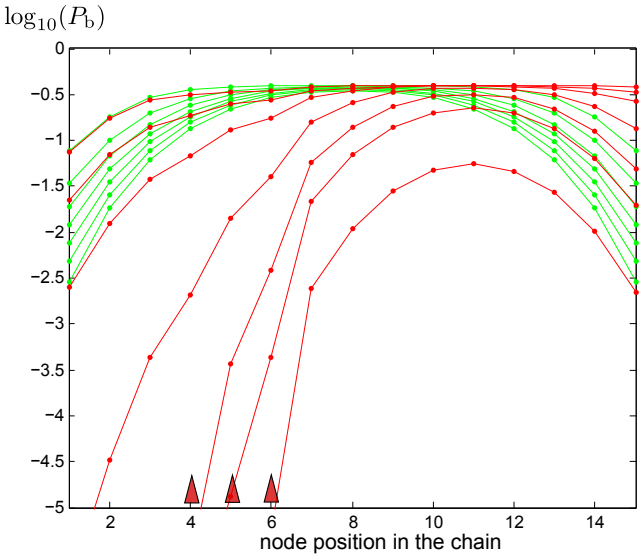

Fig. 9. Logarithm of the bit error probability for the variable nodes of the first chain of the ensembles $\mathcal{L}(3, 6, 15)$ (red curves) and $\mathcal{C}(3, 6, 15)$ (green curves), as a function of the position of the node in the chain. The curves (either red or green) are computed for decoding iterations $1, 6, 11, \ldots, 36$ (from top to bottom). The three positions where the 1st chain is connected to the end of the 2nd chain are shown by the red triangles.

B. Minimum distance analysis

In [17], Divsalar presented a technique to calculate the average weight enumerator for protograph-based block code ensembles. This weight enumerator can be used to test if an ensemble is *asymptotically good*, i.e., if the minimum distance typical of most members of the ensemble is at least as large as $\delta_{min} n$, where $\delta_{min} > 0$ its the *minimum distance growth rate* of the ensemble and n is the block length. In [18], it was shown that ensembles of (J, K)-regular SC-LDPCs (i.e., individual chains) are asymptotically good. In Section IV, we present the results of a similar protograph-based analysis for ensembles of connected SC-LDPCs to see if they share the good distance properties of the individual chains.

IV. Results

In this section we present the results on the iterative decoding thresholds and the minimum distance growth rates of the connected ensembles $\mathcal{L}(3, 6, L)$, $\mathcal{T}(3, 6, L)$, and $\mathcal{L}(3, 6, 4, 8, L)$.

A. The Loop and The Triangle Ensembles

The BEC thresholds ϵ^* for the $\mathcal{L}(3, 6, L)$ ensembles, where $L = 12, 15$, and 18, are shown in Table I. The thresholds of the single chain SC-LDPC protograph ensembles of the same rates are presented for comparison. It can be observed that the thresholds of the connected ensembles are always larger than the thresholds of the corresponding (equal rate) single chain ensembles. The largest observed improvement in the threshold happens for the rate $R = 0.4167$.

Threshold computations show that the best results are achieved for the case when the chains are connected to

Rate	Ensemble	ϵ^*	Ensemble	ϵ^*
0.4167	$\mathcal{L}(3,6,12)$	0.5237	$\mathcal{C}(3,6,12)$	0.495
0.4333	$\mathcal{L}(3,6,15)$	0.5105	$\mathcal{C}(3,6,15)$	0.489
0.4444	$\mathcal{L}(3,6,18)$	0.4989	$\mathcal{C}(3,6,18)$	0.488

TABLE I
BEC THRESHOLDS ϵ^* FOR SEVERAL SC-LDPCC ENSEMBLES $\mathcal{L}(3,6,L)$ AND SINGLE CHAIN ENSEMBLES $\mathcal{C}(3,6,L)$.

each other at the points $L/3$, i.e., when the sides of the inner loop are of length $2L/3$. To illustrate the reason for this behavior we have compared the evolution of the error probability as a function of the decoding iteration number for the ensembles $\mathcal{L}(3,6,15)$ and $\mathcal{L}'(3,6,15)$. We consider communication over the BEC with erasure probability equal to 0.5. In Fig. 10, the error probability curves, plotted for iterations $1,6,11,\ldots,36$, are presented in red for $\mathcal{L}(3,6,15)$ and in green for $\mathcal{L}'(3,6,15)$. The red triangles show the positions at which the chain connection occurs in the ensemble $\mathcal{L}(3,6,15)$. The green triangles show the positions of the chain connection for $\mathcal{L}'(3,6,15)$. We notice that the green curves show slow convergence to low error probability values, due to the fact that the connection point is located too far from the end of the chain. Therefore, the convergence advantage obtained from the connection is insufficient to boost the convergence during the early iterations (when help is most needed).

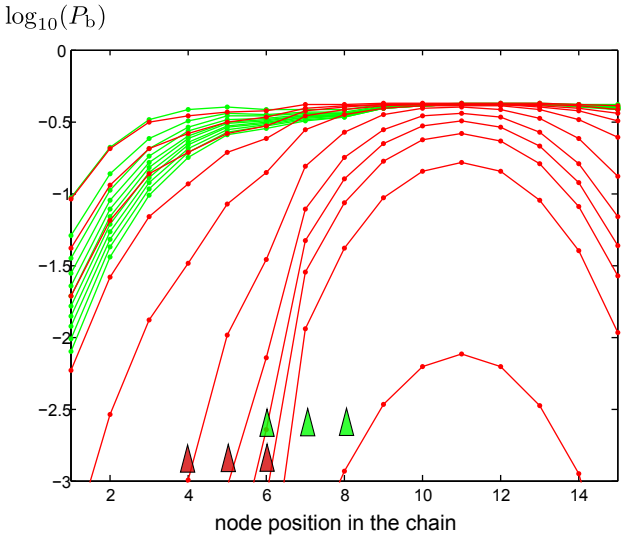

Fig. 10. Logarithm of the bit error probability for the variable nodes of the first chain of the ensembles $\mathcal{L}(3,6,15)$ (red curves) and $\mathcal{L}'(3,6,15)$ (green curves) as a function of the position of the node in the chain. The curves (either red or green) are computed for decoding iterations $1,6,11,\ldots,36$ (from top to bottom). The three positions where the first chain is connected to the end of the other chain are shown by red triangles and green triangles, respectively.

The normalized asymptotic minimum distance growth coefficients computed for the ensembles $\mathcal{L}(3,6,L)$ are given in Table II. We observe that, in addition to improved iterative decoding thresholds in comparison to the single chains, the loop ensembles are asymptotically good, i.e., they have the property that the minimum distance grows linearly with block length. Note that the growth rates decrease as the loop lengths, and correspondingly the ensemble design rates, increase. This is analogous to the effect observed by increasing the length of the single chain ensemble $\mathcal{C}(3,6,L)$ (see [18]).

L	Rate	δ_{min}
12	0.4167	0.0109
15	0.4333	0.0085
18	0.4444	0.0071

TABLE II
MINIMUM DISTANCE GROWTH RATES FOR SEVERAL $\mathcal{L}(3,6,L)$ ENSEMBLES.

Our computations show that the iterative decoding thresholds of the $\mathcal{T}(3,6,L)$ ensemble are the same as for the $\mathcal{L}(3,6,L)$ ensemble for both the BEC and the AWGN channel for a fixed chain length L. Moreover, the distance growth rates for the $\mathcal{T}(3,6,L)$ ensemble equal the corresponding growth rates of the $\mathcal{L}(3,6,L)$ ensemble when multiplied by $3/2$. These results reflect the similarity of the triangle and the loop constructions.

B. The Mixed Loop Ensemble

The BEC iterative decoding thresholds of the two mixed loop ensembles are given in Table III for $L = 15$. We notice that the thresholds of both $\mathcal{L}_1(3,6,4,8,15)$ and $\mathcal{L}_2(3,6,4,8,15)$ are better than the thresholds of single chains of the same rate. On the other hand, the threshold of the ensemble $\mathcal{L}_2(3,6,4,8,15)$ (with optimized connections) is significantly better than the threshold of the ensemble $\mathcal{L}_1(3,6,4,8,15)$, whose construction mimics the $\mathcal{L}(3,6,15)$ loop. The placement of the connections in $\mathcal{L}_2(3,6,4,8,15)$ takes into account the difference in the behavior of the connected chains. The first 6 connections from the end of the $(4,8)$ chain connect to the end of the $(3,6)$ chain to help its convergence, while the other 6 connections are placed nearly at the end of the $(3,6)$ chain where it, in turn, connects to the $(4,8)$ chain. As a result, the second set of 6 connections provides help for the convergence of the $(4,8)$ chain. This is important because the $(4,8)$ chain requires a stronger convergence boost to display threshold improvement.

Ensemble	ϵ^*
$\mathcal{L}_1(3,6,4,8,15)$	0.4997
$\mathcal{L}_2(3,6,4,8,15)$	0.5105
$\mathcal{C}(3,6,12)$	0.495
$\mathcal{C}(4,8,18)$	0.4977

TABLE III
BEC THRESHOLDS ϵ^* FOR THE MIXED LOOP ENSEMBLES AND THE SINGLE CHAIN ENSEMBLES OF THE SAME RATE.

Besides threshold improvement, connected chain constructions can also provide a reduction in decoding complexity. The average number of updates per node required to achieve a bit error probability of 10^{-5} are plotted in Fig. 11 for the mixed loop ensemble $\mathcal{L}_2(3,6,4,8,15)$ (blue curve) as well as two single chains of the same rate, the $\mathcal{C}(3,6,12)$ ensemble (red curve) and the $\mathcal{C}(4,8,18)$ ensemble (green curve). Communication over the BEC is assumed and the curves are plotted as a function of the channel erasure probability ϵ. A

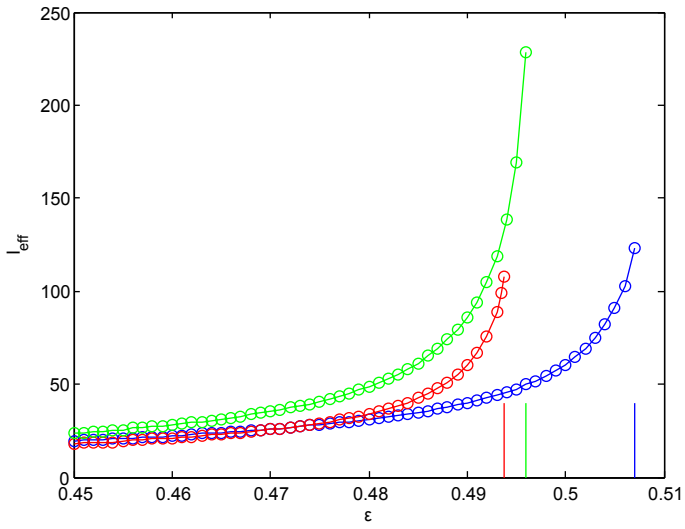

Fig. 11. The average number of updates per node I_{eff} as a function of the BEC parameter ϵ for the $\mathcal{L}_2(3,6,4,8,15)$ ensemble (blue curve), the $\mathcal{C}(3,6,12)$ ensemble (red curve) and the $\mathcal{C}(4,8,18)$ ensemble (green curve). The updating schedule with improvement constraint $\theta = 0.005$ has been used. Corresponding thresholds (for $\theta = 0.005$) are given by vertical lines.

reduced complexity update schedule with $\theta = 0.005$ has been employed. We observe that the mixed loop required a smaller number of updates to achieve the same bit error probability as the channel erasure probability ϵ approaches the limiting threshold values. These results imply that interconnecting the chains into a loop improves the convergence dynamics.

V. Conclusions

The connection of regular SC-LDPC protograph chains provides an approach to extending the spatial graph coupling phenomenon from simple (single chain) graph coupling to more general coupled structures. We have demonstrated that connecting coupled chains can result in a protograph-based LDPC code ensemble with improved thresholds and reduced iterative decoding complexity. In addition, the proposed connected protograph ensembles also achieve linear minimum distance growth. There are many possible variations on this construction method and our results indicate that the performance is sensitive to various parameters, such as the distances between connection points, the placement of connecting edges, and the individual characteristics of the component chains.

References

[1] R. G. Gallager, "Low Density Parity Check Codes", M.I.T. Press, 1963.

[2] A. Jiménez Felström and K. Sh. Zigangirov, "Time-varying periodic convolutional codes with low-density parity-check matrices," *IEEE Trans. Inf. Theory*, vol. 45, no. 6, pp. 2181–2191, Sept. 1999.

[3] S. Kudekar and H. D. Pfister, "The effect of spatial coupling on compressive sensing," in *Proc. Allerton Conf. on Communications, Control, and Computing*, Monticello, IL, Sept. 2010.

[4] C. Schlegel and D. Truhachev, "Multiple Access Demodulation in the Lifted Signal Graph with Spatial Coupling," in *Proc. IEEE Int. Symp. on Inf. Theory*, St. Petersburg, Russia, Aug. 2011.

[5] K. Takeuchi, T. Tanaka, and T. Kawabata, "Improvement of BP-based CDMA multiuser detection by spatial coupling," in *Proc. IEEE Int. Symp. on Inf. Theory*, St. Petersburg, Russia, Aug. 2011.

[6] M. Hagiwara, K. Kasai, H. Imai, and K. Sakaniwa, "Spatially coupled quasi-cyclic quantum LDPC codes," in *Proc. IEEE Int. Symp. on Inf. Theory*, St. Petersburg, Russia, Aug. 2011.

[7] S. H. Hassani, N. Macris, and R. Urbanke, "Coupled graphical models and their thresholds," in *Proc. IEEE Inf. Theory Workshop*, Dublin, Ireland, Oct. 2010.

[8] M. Lentmaier, G. P. Fettweis, K. Sh. Zigangirov, and D. J. Costello, Jr., "Approaching capacity with asymptotically regular LDPC codes," in *Proc. Inf. Theory and App. Workshop*, San Diego, CA, Feb. 2009.

[9] M. Lentmaier, A. Sridharan, D. J. Costello, Jr., and K. Sh. Zigangirov, "Iterative decoding threshold analysis for LDPC convolutional codes," *IEEE Trans. Inf. Theory*, vol. 56, no. 10, pp. 5274–5289, Oct. 2010.

[10] M. Lentmaier, D. G. M. Mitchell, G. P. Fettweis, and D. J. Costello, Jr., "Asymptotically good LDPC convolutional codes with AWGN channel thresholds close to the Shannon limit," in *Proc. 6th Int. Symp. on Turbo Codes and Iterative Inf. Processing*, Brest, France, Sept. 2010.

[11] S. Kudekar, C. Méasson, T. Richardson, and R. Urbanke, "Threshold saturation on BMS channels via spatial coupling," in *Proc. 6th Int. Symp. on Turbo Codes and Iterative Inf. Processing*, Brest, France, Sept. 2010.

[12] S. Kudekar, T. J. Richardson, and R. L. Urbanke, "Threshold saturation via spatial coupling: why convolutional LDPC ensembles perform so well over the BEC," *IEEE Trans. Inf. Theory*, vol. 57, no. 2, pp. 803–834, Feb. 2011.

[13] G. E. Corazza, A. R. Iyengar, M. Papaleo, P. H. Siegel, A. Vanelli-Coralli, and J. K. Wolf, "Latency constrained protograph-based LDPC convolutional codes," in *Proc. 6th Int. Symp. on Turbo Codes and Iterative Inf. Processing*, Brest, France, Sept. 2010.

[14] D. Truhachev, "Achieving Gaussian Multiple Access Channel Capacity With Spatially Coupled Sparse Graph Multi-User Modulation," *Proc. Inf. Theory and Applications Workshop 2012*, San Diego, USA, Feb. 2012.

[15] M. Lentmaier, M. M. Prenda, and G. Fettweis, "Efficient message passing scheduling for terminated LDPC convolutional codes," in *Proc. IEEE Int. Symp. on Inf. Theory*, St. Petersburg, Russia, Aug. 2011.

[16] J. Thorpe, "Low-density parity-check (LDPC) codes constructed from protographs," Jet Propulsion Laboratory, Pasadena, CA, INP Progress Report 42-154, Aug. 2003.

[17] D. Divsalar, "Ensemble weight enumerators for protograph LDPC codes," in *Proc. IEEE Int. Symp. on Inf. Theory*, Seattle, WA, July 2006.

[18] M. Lentmaier, D. G. M. Mitchell, G. P. Fettweis, and D. J. Costello, Jr., "Asymptotically regular LDPC codes with linear distance growth and thresholds close to capacity," in *Proc. Inf. Theory and App. Workshop*, San Diego, CA, Feb. 2010.